Dynamics of Atmospheres and Oceans 72 (2015) 52–61

Contents lists available at ScienceDirect

Dynamics of Atmospheres and Oceans

journal homepage: www.elsevier.com/locate/dynatmoce

Modulation of decadal ENSO-like variation by effective solar radiation

Fei Liu[a,b], Jing Chai[a,b], Gang Huang[c,d,*], Jian Liu[e], Zaoyang Chen[a,b]

[a] Earth System Modeling Center, Climate Dynamics Research Center, Nanjing University of Information Science and Technology, Nanjing, China
[b] Collaborative Innovation Center on Forecast and Evaluation of Meteorological Disasters, Nanjing University of Information Science and Technology, Nanjing, China
[c] State Key Laboratory of Numerical Modeling for Atmospheric Sciences and Geophysical Fluid Dynamics, Institute of Atmospheric Physics, Chinese Academy of Sciences, Beijing 100029, China
[d] Joint Center for Global Change Studies (JCGCS), Beijing 100875, China
[e] Key Laboratory of Virtual Geographic Environment of Ministry of Education, School of Geography Science, Nanjing Normal University, Nanjing 210023, China

ARTICLE INFO

Article history:
Received 26 May 2015
Received in revised form 22 October 2015
Accepted 23 October 2015
Available online 30 October 2015

Keywords:
Decadal ENSO
Effective solar radiation
Volcanic eruption

ABSTRACT

Prediction of the Pacific sea surface temperature (SST) anomaly in the coming decades is a challenge as the SST anomaly changes over time due to natural and anthropogenic climate forcing. The climate changes in the mid-1970s and late-1990s were related to the decadal Pacific SST variability. The changes in the mid-1970s were associated with the positive phase of decadal El Niño-Southern Oscillation (ENSO)-like SST variation, and the changes in the late-1990s were related to its negative phase. However, it is not clear whether this decadal SST variability is related to any external forcing. Here, we show that the effective solar radiation (ESR), which includes the net solar radiation and the effects of volcanic eruption, has modulated this decadal ENSO-like oscillation. The eastern Pacific warming (cooling) associated with this decadal ENSO-like oscillation over the past 139 years is significantly related to weak (strong) ESR. The weak ESR with strong volcanic eruption is found to strengthen the El Niño, resulting in an El Niño-like SST anomaly on the decadal time scale. The strong eruptions of the El Chicho'n (1982) and Pinatubo (1991) volcanoes reduced the ESR during the 1980s and 1990s, respectively. The radiation reduction weakened the Walker circulation due to the "ocean thermostat" mechanism that generates eastern Pacific warming associated with a decadal El Niño-like SST anomaly. This mechanism has been confirmed by the millennium run of ECHO-G model, in which the positive eastward gradient of SST over the equatorial Pacific was simulated under the weak ESR forcing on the decadal time scale. We now experience a reversal of the trend in the ESR. The strong solar radiation and lack of strong volcanic eruptions over the past 15 years have resulted in strong ESR, which should enhance the Walker circulation, leading to a La Niña-like SST anomaly.

* Corresponding author. Tel.: +86-10-82995312.
E-mail address: hg@mail.iap.ac.cn (G. Huang).

http://dx.doi.org/10.1016/j.dynatmoce.2015.10.003
0377-0265/

1. Introduction

Greenhouse gasses are known to cause centennial global warming and reduce the strength of the tropical Pacific Walker circulation (Held and Soden, 2006; Vecchi et al., 2006). The Pacific Walker circulation, which is associated with the zonal gradient of the tropical Pacific sea surface temperature (SST) anomaly, has a natural inter-decadal oscillation (Zhang et al., 1997; Vecchi et al., 2006) with global impacts (Horel and Wallace, 1981; Kousky et al., 1984; Meehl and Hu, 2006); the Walker circulation change contributes to the inter-decadal shift of the climate in the mid-1970s and late-1990s (Wang and Mehta, 2008; Meehl et al., 2009b; Wang et al., 2013).

This inter-decadal variation of the Pacific Walker circulation, which was associated with eastern Pacific warming from the mid-1970s to the late-1990s and with eastern Pacific cooling in the last 15 years, is related to the negative and positive phases of the mega El Niño-Southern Oscillation (ENSO) (Wang et al., 2013), which is referred to as the decadal ENSO (Zhang et al., 1997), the Pacific Decadal Oscillation (Mantua and Hare, 2002), or the Inter-decadal Pacific Oscillation (Power et al., 1999). The decadal La Niña-like SST anomaly is responsible for the recent intensification of the Northern-Hemisphere summer monsoon (Wang et al., 2013) and for the frequent occurrence of the Central Pacific El Niño (Xiang et al., 2013).

Whereas many studies emphasized that the decadal ENSO-like variation could be generated through an internal process of atmosphere-ocean coupling (Timmermann and Jin, 2002; Rodgers et al., 2004; Dewitte et al., 2007; Choi et al., 2009), some studies demonstrated the importance of external forcing on this decadal variation. Solar radiation and volcanic eruption are important natural forcing that acts upon the earth system and are represented by the effective solar radiation (ESR) (Crowley, 2000). The solar radiation change can force the decadal variability of the Pacific SST anomaly, and the eastern Pacific SST is found to be colder during the peak of the 11-year solar cycle (Meehl et al., 2009a). On the decadal time scale, recent simulations argued that volcanic eruptions could induce a La Niña-like response (Otterå et al., 2010; Wang et al., 2012; Zanchettin et al., 2012). The negative radiative forcing trends from volcanic eruptions are also found to cause the recent global warming hiatus (Santer et al., 2014, 2015), and this warming hiatus is found to be related to the La Niña-like SST anomaly (Kosaka and Xie, 2013). These results mean that both strong solar radiation and large explosive volcanism tend to induce the La Niña-like response on the decadal time scale. However, there is an opposite view on the total natural forcing. The strong ESR with strong solar radiation and weak volcanic eruptions will excite the tropical Pacific zonal SST gradient increases with a La Niña-like pattern and anomalous east wind stress (Liu et al., 2013; Song and Yu, 2015), which means that the weak ESR with large volcanic eruptions induces an El Niño-like pattern. Thus, it is necessary to reexamine the effect of the ESR change (composed of the net solar radiation and effects of volcanic eruption) on the decadal variability of the equatorial Pacific SST anomaly.

A detailed description of the data and methodology is presented in Section 2. In Section 3 the external forcing is presented. We discuss the spatial distribution of the decadal Pacific SST variability and its relation to the ESR in Section 4. Model simulation is used to prove the effect of the ESR in Section 5. The main results are summarized in Section 6.

2. Data and method

To analyze the decadal variability, two sets of long-term SST data for 1870–2008 were used in this study. One dataset is the interpolated monthly mean SST obtained from the extended reconstructed sea surface temperatures (ERSST, version 3b) (Smith et al., 2008). Because the Hadley Centre Ice and SST (version 1; HadISST1) includes artificial trends that are inappropriate for analysing long-term trends (Deser et al., 2010; Tokinaga et al., 2012), the un-interpolated HadISST2 was also used (Rayner et al., 2006). The monthly mean precipitation was obtained from the merged statistical analyses of historical monthly precipitation anomalies (20C RECG) at a 2.5° spatial resolution for the period from 1900 to 2008 (Smith et al., 2010).

Outputs from the millennial simulation of the ECHO-G model (Zorita et al., 2005) were analyzed. This forced run, named ERIK, covering the period AD 1000–1990, is externally forced by solar variability, effective radiative effects from stratospheric volcanic aerosols, and greenhouse-gas concentrations in the atmosphere, including CO_2 and CH_4, for the period AD 1000–1990.

The annual mean of external forcing data was used. Since the SST anomaly associated with the ENSO is strong during boreal winter time, the boreal winter averaged (November-March) SST and precipitation anomalies were studied. To study the decadal variability, a simple low-pass filter, i.e., a 5-year running mean, was applied. The half-point of the response function for this 5-year running mean was approximately 10 years; thus, it largely removed the interannual ENSO signal that has a periodicity of 2–7 years. To identify the decadal variation mode, a principal-component (PC) analysis of the smoothed SST was performed. For two time series (X and Y) with smoothing, we must calculate the effective degree of freedom. Following Livezey and Chen (1983), a measure of the effective time between independent samples can be estimated from the autoregressive properties of both time series.

$$\tau = \left[1 + 2\sum_{i=1}^{N} C_{XX}(i\Delta t)\, C_{YY}(i\Delta t)\right] \Delta t, \tag{1}$$

where Δt is the sampling time, N is the number of samples, and Cs are the autocorrelations at lag $i\Delta t$ for the time series. From τ, the effective number of independent samples (or effective degree of freedom) in the time series $\tau = N\Delta t/\tau$ can be determined. The Student t-test for assessing significance is

$$t = \frac{r\sqrt{\tau - 2}}{\sqrt{1 - r^2}}, \tag{2}$$

where r is Pearson's correlation coefficient.

We use superposed epoch analysis (Haurwitz and Brier, 1981) to evaluate the influence of the explosive volcanic eruption on the global SST and precipitation anomalies. A conventional bootstrapped resampling with replacement is used, and the confidence intervals are calculated by repeating the superposed epoch analysis using repeated (n = 10,000) random draws of pseudo—"event" year from the available time span. Significance is then evaluated by comparing percentiles from the random draw to the composite mean of the real data. Following Adams et al. (2003) and Anchukaitis et al. (2010), we normalized the data in the event window by each volcanic strength to avoid the possibility that any single eruption would dominate the epochal signal.

3. External forcing

The ESR was obtained from the dataset reconstructed by Crowley (2000); the data ended in 1990. To include climate change over the past decade, we must extend the data. Here, the net radiation data (Lean, 2000) and volcanic eruption data (Gao et al., 2008) from 1979 to 2008 are used (Fig. 1). Because the solar radiation datasets of Lean and Crowley have a systematic bias of 1.5 W m^{-2} and different variation (Crowley, 2000; Lean, 2000), we projected the solar radiation data of Lean onto that of Crowley after adding a mean of 1.5 W m^{-2} and by amplifying the variation by a factor of 1.5. In the work of Crowley (2000), the volcanic forcing was parameterized as a simple reduction of the annual mean solar constant over a couple of years, which began in a year with a volcanic eruption. In the past 30 years (1979–2008), two large volcanic eruptions had strong effects on the solar radiation (Gao et al., 2008), i.e., El Chichón (14 Tg) and Pinatubo (31 Tg), which erupted in 1982 and 1991, respectively. We project these two eruptions based on the data of Crowley; the value proposed by Crowley was also used for 1982, and a larger value (a ratio of 31/14 relative to 1982) was used for 1991. During 1979–2008, the volcanic eruption effect was zero for all the other years. The CO_2 emission data after 1979 originated from the Scripps Institution of Oceanography (Keeling et al., 2001). We reconstructed the ESR and CO_2 data by extending the data of Crowley.

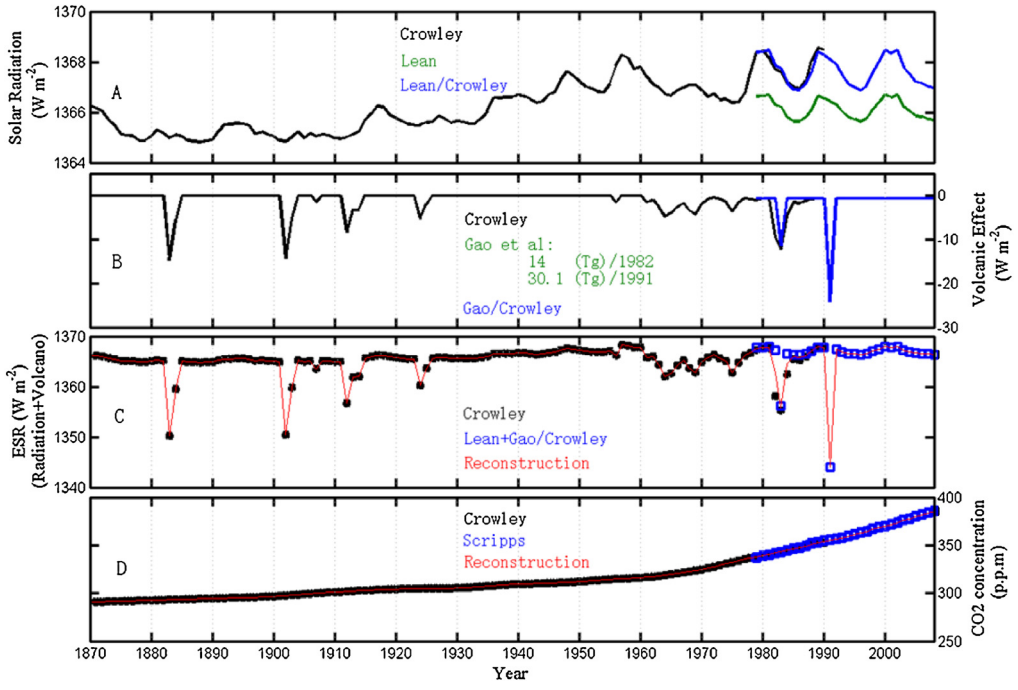

Fig. 1. External forcing. (A) Solar radiation data are obtained from Crowley (black; 2000) and Lean (green; 2000). The blue line represents the projected solar radiation of Lean onto that of Crowley. (B) The black line is the volcanic eruption effect obtained by Crowley, and the blue line is the projected effect of the eruption data of Gao et al. (2008) onto that of Crowley. (C) The effective solar radiation (ESR; including effects of solar radiation and volcanic eruption) of Crowley (black), the projected data (blue) and the reconstructions (red). (D) CO_2 emission data from Crowley (black), Scripps (blue) (Keeling et al., 2001)and the reconstructions (red) (p.p.m. = parts per million). (For interpretation of the references to colour in this figure legend, the reader is referred to the web version of this article.)

The data of Crowley were used for 1870–1978; the average of Crowley and the projected data of Lean (2000) and Gao et al. (2008), as well as the Scripps Institution of Oceanography, were used for 1979–1990; and the projected data were used for the last 18 years (1991–2008).

Based on Fig. 1A, the solar radiation increased over the past 139 years, mainly during 1930 to 1960. During that time, volcanic eruptions were weak (Fig. 1B), and the strong volcanic eruptions during the late 19th and late 20th centuries dramatically reduced the ESR (Fig. 1C). Thus, the ESR experienced significant decadal variability with lower values during 1880–1920 and 1960–1995 and higher values during 1930–1960 and 1995–2008. The CO_2 emissions only showed a monotonic increase (Fig. 1D).

4. Decadal ENSO-like variation

The global SST anomalies based on the ERSST mainly show two leading Empirical Orthogonal Function (EOF) modes, which are easily distinguished from the higher modes (not shown). The first EOF mode, which shows global warming (Fig. 2A), is highly correlated to the CO_2 emissions (Fig. 2C). The second EOF mode (Fig. 2B), which shows a La Niña-like SST anomaly, is identified as the decadal ENSO-like mode, whose index can be represented by PC2 (Wang et al., 2013). The global mean SST of EOF2, however, is very small (−0.01 °C) compared to that of EOF1 (0.28 °C), which means that EOF2 only contributes to a very small portion of the global mean SST anomaly.

Strikingly, PC2 is significantly correlated to the ESR (Fig. 2C; $r = 0.53$, $p < 0.01$, and $n_{edof} = 29$, which is the effective degree of freedom). This positive correlation means that the decadal La Niña-like pattern is associated with the enhanced ESR. From the late-1970s to the late-1990s, the ESR had low values due to the eruptions of the strong volcanoes of El Chicho'n and Pinatubo in 1982 and 1991, when the eastern Pacific was in a warm El Niño-like phase. Since the mid-1990s, no strong volcanic eruptions occurred (Fig. 1B), while the net solar radiation was strong (Fig. 1A); thus, the ESR was enhanced and the Pacific entered a decadal La Niña-like phase, which was accompanied by enhanced precipitation over the Indo-Pacific warm pool region (Fig. 3 B). Although the CO_2 emissions increased the global mean SST, precipitation was enhanced over the equatorial Pacific but reduced over the Indo-Pacific warm pool region (Fig. 3A); the global circulation weakened due to this anthropogenically induced warming (Vecchi and Soden, 2007). The equatorial zonal SST gradient was dominated by the decadal ENSO-like variability.

The HadISST2 dataset was also studied. Because the HadISST2 is un-interpolated, we mainly examined the Niño-3.4 SST anomaly, which represents the ENSO strength. The Niño-3.4 is defined by the area (120°W–170°W, 5°S–5°N) averaged SST anomaly. Associated with the increasing CO_2 emissions, the Niño-3.4 of the two datasets show significant increases; the increase in the ERSST is stronger than that in the HadISST2 (Fig. 4). After removing this increase, the detrended Niño-3.4

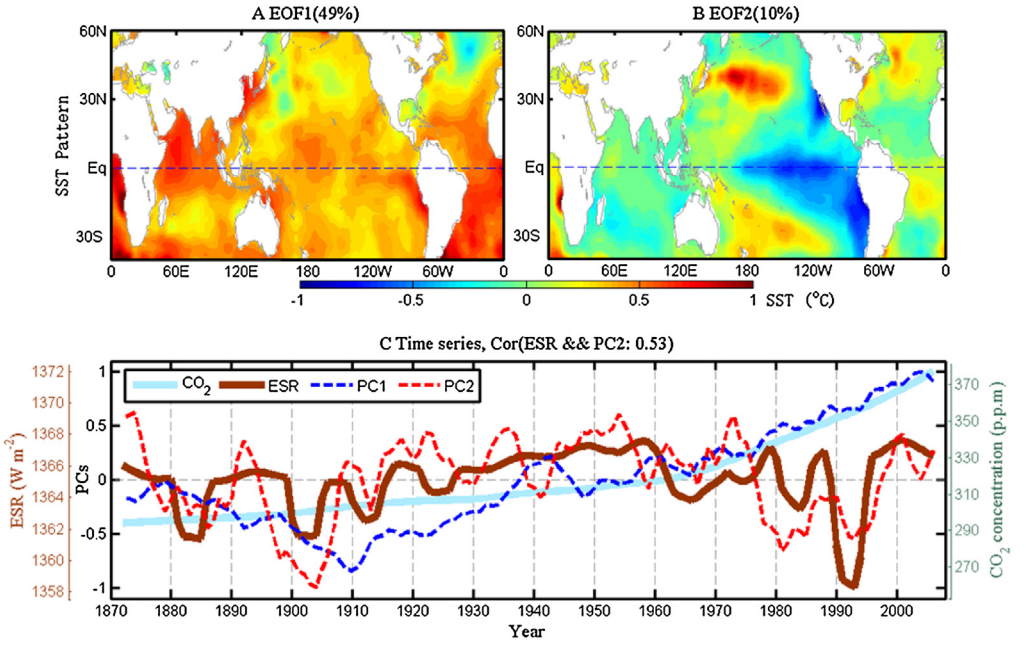

Fig. 2. Spatial patterns and time series with reference to CO_2 and ESR forcing. The SST anomalies are shown for the first EOF (A) and the second EOF (B) based on the ERSST; the first two EOFs explain 49% and 10% of the total variance, respectively. (C) The time series of the reconstructed CO_2 emissions (solid light blue), ESR (solid dark red), PC1 (dashed blue), and PC2 (dashed red). Five-year running mean is used for all data over 1870–2008. A cosine area weighting was applied in the EOF analysis. The global mean SSTs of (A) and (B) are 0.28 °C and −0.01 °C, respectively. (For interpretation of the references to colour in this figure legend, the reader is referred to the web version of this article.)

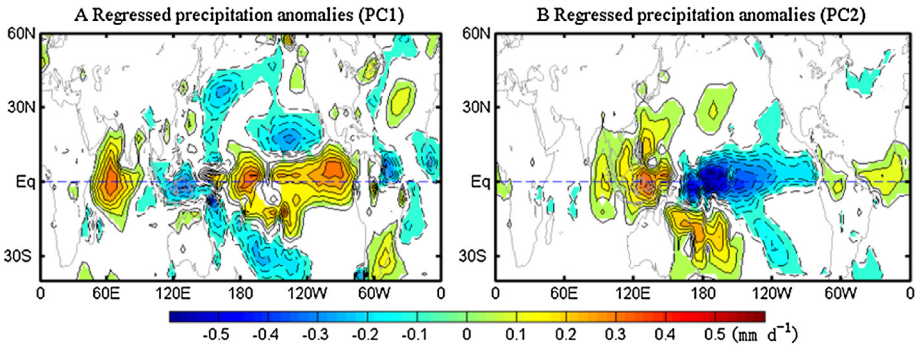

Fig. 3. Spatial patterns of precipitation anomalies regressed to (A) PC1 and (B) PC2 during 1900–2008 shown in Fig. 2. The positive (negative) anomalies are represented by solid (dashed) contours, and the precipitation contour interval is 0.05 mm d^{-1}. The shaded anomalies are significant above the 95% confidence level. Five-year running mean was applied.

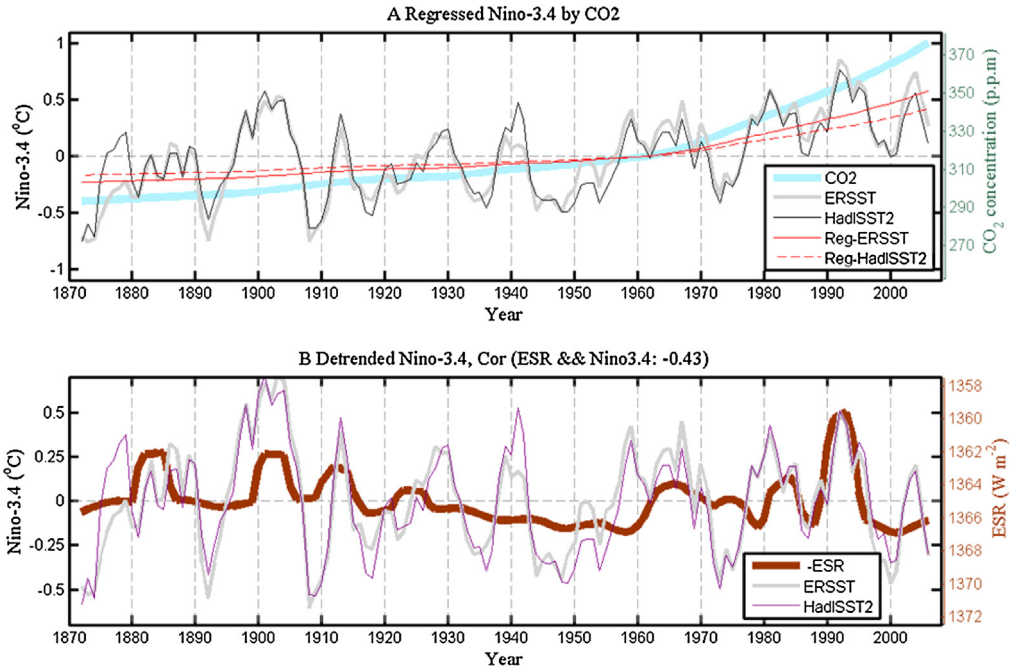

Fig. 4. Relation among Niño-3.4, CO_2 and ESR forcing. (A) The time series of the reconstructed CO_2 emissions (blue), Niño-3.4 in the ERSST (thick grey), Niño-3.4 in the HadISST2 (dark), and regressed Niño-3.4 to CO_2 in the ERSST (solid red) and to the HadISST2 (dashed red). (B) The time series of the ESR (solid maroon) and detrended Niño-3.4 by removing the regressed Niño-3.4 to CO_2 in the ERSST (grey) and in the HadISST2 (purple). Five-year running mean was applied to all the data over 1870–2008. (For interpretation of the references to colour in this figure legend, the reader is referred to the web version of this article.)

in the two datasets agreed well; both datasets are significantly correlated to the ESR ($r = -0.43$, $p < 0.05$, and $n_{edof} = 27$ for average of two datasets).

The ESR was largely controlled by five strong volcanic eruptions over the past 139 years, which occurred in 1883, 1902, 1912, 1982, and 1991. The enhanced probability of La Niña was found within one year of a large eruption (McGregor and Timmermann, 2011), while Ohba et al. (2013) found the opposite response. In recent research, a large volcanic eruption was found to increase the occurrence of El Niño, which only lasted one or two years (Li et al., 2013). Our results support the latter (Fig. 5A), in which a significant El Niño-like SST pattern was excited lasting three years after the volcanic eruption. The 10-year-averaged SST anomaly also has a significant El Niño-like pattern after the strong volcanic eruption (Fig. 5B), which means that the recent strong El Chicho'n (1982) and Pinatubo (1991) volcanoes would reduce the ESR and induce the decadal El Niño-like SST anomalies during the late-1970s and late-1990s.

We further analyze the Niño-3.4 SST anomaly related to the ESR change, including the strong volcano variability (Fig. 6). Both ERSST and HadISST2 gave similar results. When a volcano erupted, the ensemble mean Niño-3.4 showed that a warm El Niño-like set-up. Year 0 denotes the year when the volcanic eruption occurred. Since we studied the boreal winter from November of the eruption year to March of the following year, the positive Niño-3.4 SST anomaly in the boreal winter

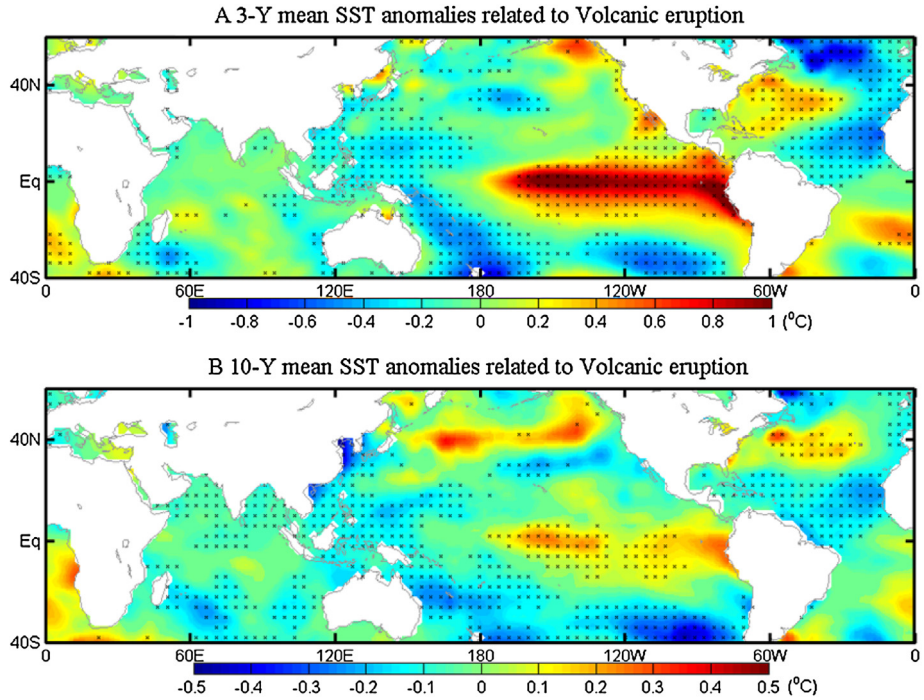

Fig. 5. Superposed Epoch Analysis of the SST after the volcanic eruptions. (A) The composite difference of the 3-year-mean SST after and before the five large volcanic eruptions since 1870 based on the ERSST. (B) Same as (A), except for the 10-year mean. The five large volcanic eruptions occurred in 1883, 1902, 1912, 1982, and 1991. Statistically significant (90% one-tailed) epochal anomalies based on the Monte Carlo resampling ($n = 10{,}000$) are indicated by crosses. The linear trend with respect to CO_2 was removed in the ERSST result.

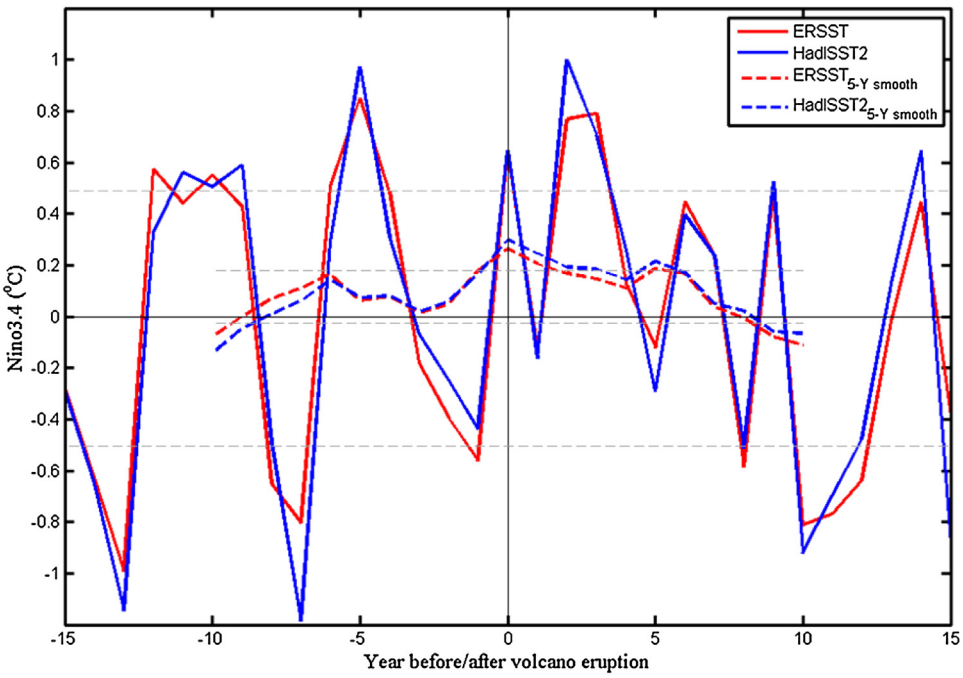

Fig. 6. Superposed Epoch Analysis using the Niño-3.4 SST anomaly related to the five strong volcanic eruptions in Fig. 5. The ensemble mean Niño-3.4 SST anomaly before and after the five strong volcanic eruptions in the ERSST (solid red) and in the HadISST2 (solid blue), as well as their 5-year running means (dashed red and blue), are shown. Significance levels (90%) derived from Monte Carlo block resampling ($n = 10{,}000$) of the actual event year windows are indicated by horizontal dashed lines in the plots for the original and smoothed Niño-3.4. The linear trend with respect to CO_2 has been removed in both ERSST and HadISST2. (For interpretation of the references to colour in this figure legend, the reader is referred to the web version of this article.)

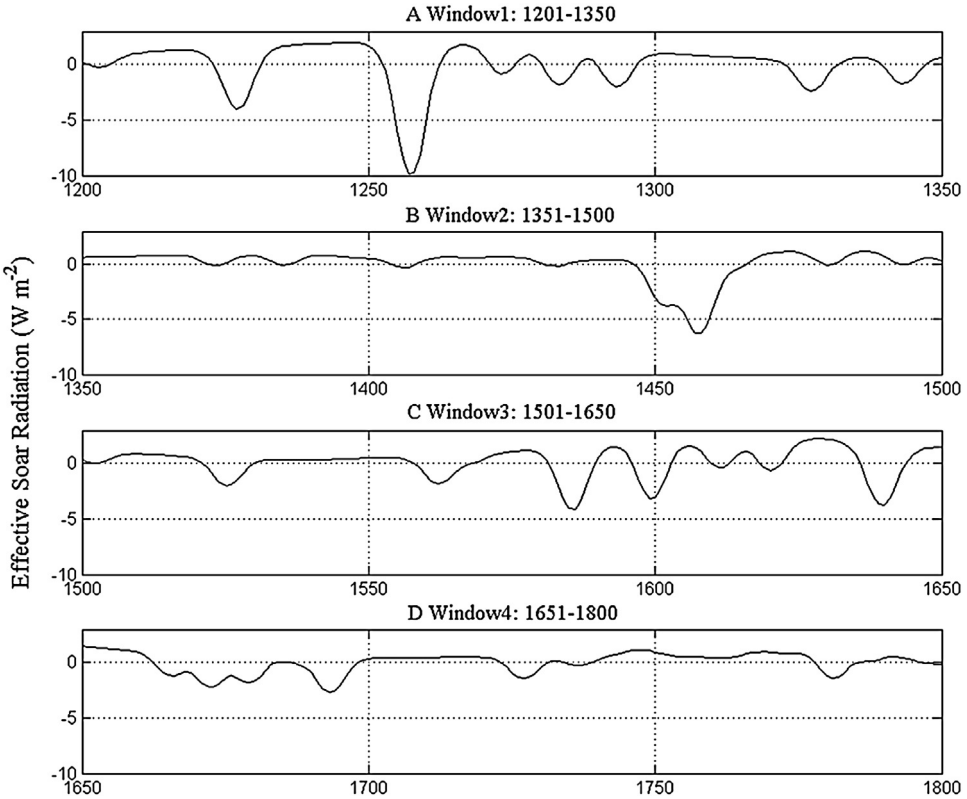

Fig. 7. External ESR used in the millennium run of ECHO-G model during four windows: (A) 1201–1350, (B) 1351–1500, (C) 1501–1650, and (D) 1651–1800. Five-year running mean was applied for each window.

already existed in the eruption year. Before the volcanic eruption, the Niño-3.4 experienced an oscillation with a period of 2-7 years; the Niño-3.4 was symmetric; thus, El Niño and La Niña had comparable amplitudes, and the Niño-3.4 on the decadal time scale should be negligible, which can be seen from their 5-year smoothing. After the volcanic eruption, the El Niño was followed by a La Niña, while the Niño 3.4 experienced a stronger positive anomaly than a negative anomaly, which can be confirmed by the significant positive Niño-3.4 SST anomaly of 5-year smoothing after the volcanic eruption. For a pure symmetrical internal oscillation, an external volcanic eruption diminished the symmetry. Here, we do not exclude the internal variability of the ENSO. We conclude that the weak ESR with strong volcanic eruption tended to strength the El Niño and induce a decadal El Niño-like SST anomaly.

Because of global warming, the zonal gradient of tropical Pacific SST increased when solar radiation increased and decreased when greenhouse gasses increased (Liu et al., 2013). The greenhouse gas effect increased atmospheric static stability and weakened tropical circulations, which were accompanied by weaker SST gradients (Fig. 2A) and negative precipitation anomalies over the Indo-Pacific warm pool region (Fig. 3A). This weak Walker circulation hypothesis is supported by the Intergovernmental Panel on Climate Change (IPCC) model projection for the 21st century (Vecchi et al., 2008). The ESR seemed to prefer the "ocean dynamical thermostat" mechanism (Clement et al., 1996; Cane et al., 1997; Bauer et al., 2003), i.e., increased heating at the surface warmed the SST in the west because the heating in the east was offset by the upwelling of cold water (Fig. 2B). The strong SST gradient produced an enhanced pressure gradient and a stronger Walker circulation, which in turn enhanced the SST gradient through the "Bjerknes feedback." As a result, strong precipitation occurred in the Indo-Pacific warm pool region (Fig. 3B). These findings support the "wet region getting wetter" argument (Held and Soden, 2006).

5. Model simulation

The effects of the ESR forcing are simulated in the millennium run during 1000–1990 by the ECHO-G model (Legutke and Voss, 1999). Details of this millennium run can be found in Liu et al. (2013). In the millennium simulation, the continuous aerosol concentration associated with the volcanic eruption was used, which could last 1-3 years for each eruption. We analyzed the simulation from 1201 to 1800 to avoid model initial response and greenhouse gas effect in the recent history. Consistent with the observation analysis, we split this 600-year simulation into four windows of 150 years each, and a 5-year running mean is performed for each window (Fig. 7).

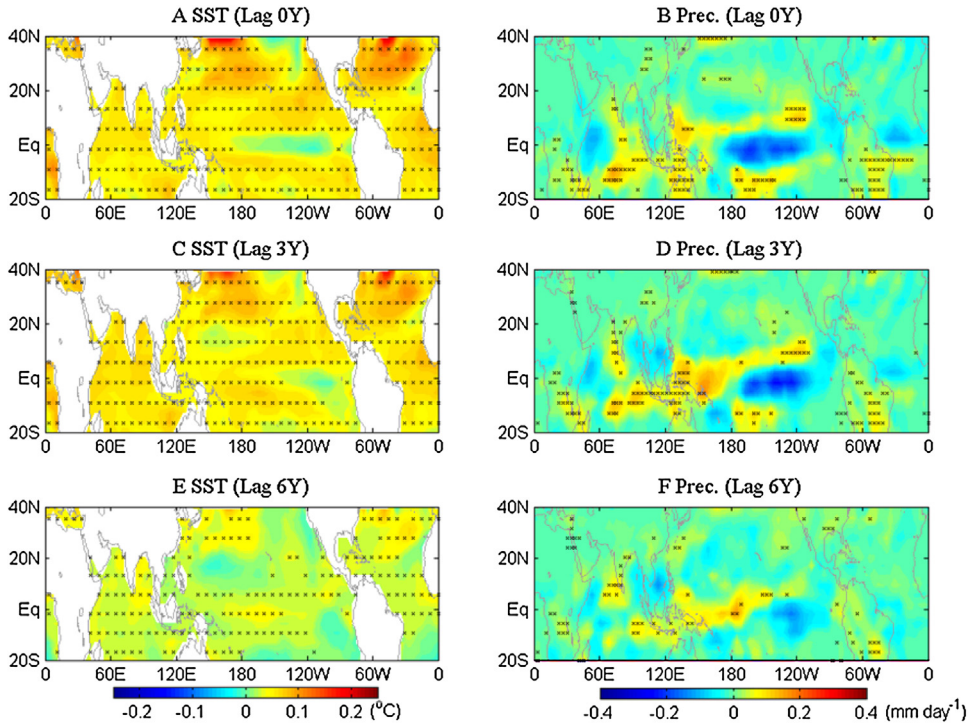

Fig. 8. ESR-induced La Niña-like pattern in the ECHO-G millennium run. Ensemble spatial patterns of (A) SST and (B) precipitation anomalies regressed to the simultaneous external ESR of each window given in Fig. 7 are shown. The shaded anomalies significant above the 95% confidence level are marked by crosses. Five-year running mean was applied for each window. (C–D) and (E–F) are the same as (A–B), except for the SST and precipitation anomalies regressed to the 3-year and 6-year lagged ESR.

Fig. 8 shows the ensemble regression of SST and precipitation anomalies of these four epochs with respect to the ESR forcing. Under the ESR forcing, though the eastern Pacific SST variability were not well simulated, the La Niña-like SST gradient and precipitation distribution, i.e., negative eastward SST gradient over the equatorial Pacific and enhanced precipitation over the Indo-Pacific warm pool region, were well simulated (Fig. 8A and B). This means that the model with weak ESR led to the El Niño-like SST gradient or positive eastward SST gradient over the equatorial Pacific. Fig. 8C–F show the lagged regression with respect to the ESR. We can see that the effect of the ESR with a strong volcanic component lasted for some years, although the effect became weaker over time after the eruption. Although the role of ESR on decadal SST variation was confirmed by the model simulation, we would like to conclude that the ESR variability is only one of the reasons for the decadal Pacific SST variation.

6. Concluding remarks

Predictions of Pacific SST in the coming decades are a challenge because SST changes involve internal natural variability, external natural (e.g., solar and volcanic activity) and anthropogenic (e.g., greenhouse gasses, aerosols and land use) climate forcing. In this study, we demonstrated that the ESR, which includes net solar radiation and volcanic eruption, is responsible for the decadal ENSO-like variation. The enhanced solar radiation and lack of large volcanic eruptions over the past 15 years increased the ESR and may have induced the recent decadal La Niña-like SST anomalies. Previous studies demonstrated that a volcanic eruption tended to affect the ENSO within a few years (Li et al., 2013; Ohba et al., 2013); our analysis showed that the weak ESR with strong volcanic eruption tended to enhance the El Niño, which resulted in a El Niño-like SST anomaly on the decadal time scale.

Over the past 15 years or so, the global warming “slow-down” or global warming “hiatus” received considerable scientific, political and media attentions. In recent years many studies have been conducted to explain the phenomenon. The global warming “hiatus” may be caused by the eastern Pacific cooling (Kosaka and Xie, 2013), which is related to the enhanced deep ocean heating (Meehl et al., 2011; Chen and Tung, 2014; Drijfhout et al., 2014), the Atlantic warming induced Pacific cooling (England et al., 2014), or the tropical Pacific easterly wind anomalies (England et al., 2014). Recent studies also showed that a series of moderate volcanic eruptions over the past 15 years contributed to the global warming “hiatus” through influencing the solar radiation (Fyfe et al., 2013; Santer et al., 2014, 2015; Schmidt et al., 2014). In our analysis, although the eastern Pacific was found to be cold associated with the enhanced ESR, the global mean SST variation associated with the ESR change was negligible (Fig. 2). Thus, we conclude that the enhanced external ESR in the recent 15 years helps to

select the La Niña-like SST anomalies, while the internal variability was also important for this decadal oscillation, and the strong internal process of the decadal La Niña-like mode transported heating into deep ocean and slowed down the global warming (Meehl et al., 2011; Drijfhout et al., 2014).

We also analyzed the simulated decadal ENSO-like variation using 20 models of the Coupled Model Intercomparison Project Phase 5 (CMIP5). The 20 models are listed in Table 1 of Lee and Wang (2014). When defining the decadal index by projecting the observed La Niña-like pattern (Fig. 2B) onto these modelled SSTs, no correlation between modelled index and observation (PC2 in Fig. 2C) is significant for any of the models. In future, it will be necessary to explain why the models cannot capture the correct phase of this decadal ENSO-like oscillation.

Acknowledgements

This work was supported by the National Natural Science Foundation of China (41420104002), the China National 973 Project (2015CB453200 and 2012CB955604), and the Natural Science Foundation of Jiangsu (BK20150907). G.H. was supported by the National Outstanding Youth Science Fund Project of China (41425019), and the National Natural Science Foundation of China (41275083 and 91337105). This paper is the ESMC Contribution No. 072.

References

Adams, J.B., Mann, M.E., Ammann, C.M., 2003. Proxy evidence for an El Nino-like response to volcanic forcing. Nature 426 (6964), 274–278.
Anchukaitis, K., Buckley, B., Cook, E., Cook, B., D'Arrigo, R., Ammann, C., 2010. Influence of volcanic eruptions on the climate of the Asian monsoon region. Geophys. Res. Lett. 37. (22), L22703, http://dx.doi.org/10.1029/2010GL044843.
Bauer, E., Claussen, M., Brovkin, V., Huenerbein, A., 2003. Assessing climate forcings of the Earth system for the past millennium. Geophys. Res. Lett. 30 (6), 1276.
Cane, M.A., Clement, A.C., Kaplan, A., Kushnir, Y., Pozdnyakov, D., Seager, R., Zebiak, S.E., Murtugudde, R., 1997. Twentieth-century sea surface temperature trends. Science 275 (5302), 957–960.
Chen, X., Tung, K.-K., 2014. Varying planetary heat sink led to global-warming slowdown and acceleration. Science 345 (6199), 897–903.
Choi, J., An, S.-I., Dewitte, B., Hsieh, W.W., 2009. Interactive feedback between the tropical Pacific decadal oscillation and ENSO in a coupled general circulation model. J. Clim. 22 (24), 6597–6611.
Clement, A.C., Seager, R., Cane, M.A., Zebiak, S.E., 1996. An ocean dynamical thermostat. J. Clim. 9 (9), 2190–2196.
Crowley, T.J., 2000. Causes of climate change over the past 1000 years. Science 289 (5477), 270–277.
Deser, C., Phillips, A.S., Alexander, M.A., 2010. Twentieth century tropical sea surface temperature trends revisited. Geophys. Res. Lett. 37, L10701.
Dewitte, B., Yeh, S.-W., Moon, B.-K., Cibot, C., Terray, L., 2007. Rectification of ENSO variability by interdecadal changes in the equatorial background mean state in a CGCM simulation. J. Clim. 20 (10), 2002–2021.
Drijfhout, S., Blaker, A., Josey, S., Nurser, A., Sinha, B., Balmaseda, M., 2014. Surface warming hiatus caused by increased heat uptake across multiple ocean basins. Geophys. Res. Lett. 41 (22), 7868–7874, http://dx.doi.org/10.1002/2014GL061456.
England, M.H., McGregor, S., Spence, P., Meehl, G.A., Timmermann, A., Cai, W., Gupta, A.S., McPhaden, M.J., Purich, A., Santoso, A., 2014. Recent intensification of wind-driven circulation in the Pacific and the ongoing warming hiatus. Nat. Clim. Change 4 (3), 222–227.
Fyfe, J., Salzen, K., Cole, J., Gillett, N., Vernier, J.P., 2013. Surface response to stratospheric aerosol changes in a coupled atmosphere–ocean model. Geophys. Res. Lett. 40 (3), 584–588.
Gao, C., Robock, A., Ammann, C., 2008. Volcanic forcing of climate over the past 1500 years: an improved ice core-based index for climate models. J. Geophys. Res. Atmos. 113 (D12), 23111.
Haurwitz, M.W., Brier, G.W., 1981. A critique of the superposed epoch analysis method: its application to solar-weather relations. Mon. Weather Rev. 109 (10), 2074–2079.
Held, I.M., Soden, B.J., 2006. Robust responses of the hydrological cycle to global warming. J. Clim. 19 (21), 5686–5699.
Horel, J.D., Wallace, J.M., 1981. Planetary-scale atmospheric phenomena associated with the Southern Oscillation. Mon. Weather Rev. 109 (4), 813–829.
Keeling, C.D., Piper, S.C., Bacastow, R.B., Wahlen, M., Whorf, T.P., Heimann, M., Meijer, H.A., 2001. Exchanges of atmospheric CO_2 and $13CO_2$ with the terrestrial biosphere and oceans from 1978 to 2000. I. Global Aspects, SIO Reference Series, No. 01-06, vol. 88. Scripps Institution of Oceanography, San Diego, CA, pp. 2001.
Kosaka, Y., Xie, S.-P., 2013. Recent global-warming hiatus tied to equatorial Pacific surface cooling. Nature 501 (7467), 403–407.
Kousky, V.E., Kagano, M.T., Cavalcanti, I.F., 1984. A review of the Southern Oscillation: oceanic–atmospheric circulation changes and related rainfall anomalies. Tellus Ser. A 36 (5), 490–504.
Lean, J., 2000. Evolution of the sun's spectral irradiance since the Maunder Minimum. Geophys. Res. Lett. 27, 2425–2428.
Lee, J.-Y., Wang, B., 2014. Future change of global monsoon in the CMIP5. Clim. Dyn. 42 (1–2), 101–119.
Legutke, S., Voss, R., 1999. The Hamburg atmosphere–ocean coupled circulation model ECHO-G. Tech. Rep. 18, 1–62.
Li, J., Xie, S.-P., Cook, E.R., Morales, M.S., Christie, D.A., Johnson, N.C., Chen, F., D'Arrigo, R., Fowler, A.M., Gou, X., 2013. El Nino modulations over the past seven centuries. Nat. Clim. Change 3 (9), 822–826.
Liu, J., Wang, B., Cane, M.A., Yim, S.-Y., Lee, J.-Y., 2013. Divergent global precipitation changes induced by natural versus anthropogenic forcing. Nature 493 (7434), 656–659.
Livezey, R.E., Chen, W., 1983. Statistical field significance and its determination by Monte Carlo techniques. Mon. Weather Rev. 111 (1), 46–59.
Mantua, N.J., Hare, S.R., 2002. The Pacific decadal oscillation. J. Oceanogr. 58 (1), 35–44.
McGregor, S., Timmermann, A., 2011. The effect of explosive tropical volcanism on ENSO. J. Clim. 24 (8), 2178–2191.
Meehl, G.A., Arblaster, J.M., Fasullo, J.T., Hu, A., Trenberth, K.E., 2011. Model-based evidence of deep-ocean heat uptake during surface-temperature hiatus periods. Nat. Clim. Change 1 (7), 360–364.
Meehl, G.A., Arblaster, J.M., Matthes, K., Sassi, F., van Loon, H., 2009a. Amplifying the Pacific climate system response to a small 11-year solar cycle forcing. Science 325 (5944), 1114–1118.
Meehl, G.A., Hu, A., 2006. Megadroughts in the Indian monsoon region and southwest North America and a mechanism for associated multidecadal Pacific sea surface temperature anomalies. J. Clim. 19 (9), 1605–1623.
Meehl, G.A., Hu, A., Santer, B.D., 2009b. The mid-1970s climate shift in the Pacific and the relative roles of forced versus inherent decadal variability. J. Clim. 22 (3), 780–792.
Ohba, M., Shiogama, H., Yokohata, T., Watanabe, M., 2013. Impact of strong tropical volcanic eruptions on ENSO simulated in a coupled GCM. J. Clim. 26 (14), 5169–5182.
Otterå, O.H., Bentsen, M., Drange, H., Suo, L., 2010. External forcing as a metronome for Atlantic multidecadal variability. Nat. Geosci. 3 (10), 688–694.
Power, S., Casey, T., Folland, C., Colman, A., Mehta, V., 1999. Inter-decadal modulation of the impact of ENSO on Australia. Clim. Dyn. 15 (5), 319–324.

Rayner, N., Brohan, P., Parker, D., Folland, C., Kennedy, J., Vanicek, M., Ansell, T., Tett, S., 2006. Improved analyses of changes and uncertainties in sea surface temperature measured in situ since the mid-nineteenth century: the HadSST2 dataset. J. Clim. 19 (3), 446–469.
Rodgers, K.B., Friederichs, P., Latif, M., 2004. Tropical Pacific decadal variability and its relation to decadal modulations of ENSO. J. Clim. 17 (19), 3761–3774.
Santer, B.D., Bonfils, C., Painter, J.F., Zelinka, M.D., Mears, C., Solomon, S., Schmidt, G.A., Fyfe, J.C., Cole, J.N., Nazarenko, L., 2014. Volcanic contribution to decadal changes in tropospheric temperature. Nat. Geosci. 7 (3), 185–189.
Santer, B.D., Solomon, S., Bonfils, C., Zelinka, M.D., Painter, J.F., Beltran, F., Fyfe, J.C., Johannesson, G., Mears, C., Ridley, D.A., 2015. Observed multivariable signals of late 20th and early 21st century volcanic activity. Geophys. Res. Lett. 42 (2), 500–509.
Schmidt, G.A., Shindell, D.T., Tsigaridis, K., 2014. Reconciling warming trends. Nat. Geosci. 7 (3), 158–160.
Smith, T.M., Arkin, P.A., Sapiano, M.R., Chang, C.-Y., 2010. Merged statistical analyses of historical monthly precipitation anomalies beginning 1900. J. Clim. 23 (21), 5755–5770.
Smith, T.M., Reynolds, R.W., Peterson, T.C., Lawrimore, J., 2008. Improvements to NOAA's historical merged land-ocean surface temperature analysis (1880–2006). J. Clim. 21 (10), 2283–2296.
Song, Y., Yu, Y., 2015. Impacts of external forcing on the decadal climate variability in CMIP5 simulations. J. Clim. 2015, http://dx.doi.org/10.1175/JCLI-D-14-00492.1.
Timmermann, A., Jin, F.-F., 2002. A nonlinear mechanism for decadal El NiñO amplitude changes. Geophys. Res. Lett. 29, 1003.
Tokinaga, H., Xie, S.-P., Deser, C., Kosaka, Y., Okumura, Y.M., 2012. Slowdown of the Walker circulation driven by tropical Indo-Pacific warming. Nature 491 (7424), 439–443.
Vecchi, G.A., Clement, A., Soden, B.J., 2008. Examining the tropical Pacific's response to global warming. Eos, Trans. Am. Geophys. Union 89 (9), 81–83.
Vecchi, G.A., Soden, B.J., 2007. Global warming and the weakening of the tropical circulation. J. Clim. 20 (17), 4316–4340.
Vecchi, G.A., Soden, B.J., Wittenberg, A.T., Held, I.M., Leetmaa, A., Harrison, M.J., 2006. Weakening of tropical Pacific atmospheric circulation due to anthropogenic forcing. Nature 441 (7089), 73–76.
Wang, B., Liu, J., Kim, H.-J., Webster, P.J., Yim, S.-Y., Xiang, B., 2013. Northern Hemisphere summer monsoon intensified by mega-El Niño/southern oscillation and Atlantic multidecadal oscillation. Proc. Natl. Acad. Sci. U.S.A. 110 (14), 5347–5352.
Wang, H., Mehta, V.M., 2008. Decadal variability of the Indo-Pacific warm pool and its association with atmospheric and oceanic variability in the NCEP-NCAR and SODA reanalyses. J. Clim. 21 (21), 5545–5565.
Wang, T., Otterå, O.H., Gao, Y., Wang, H., 2012. The response of the North Pacific Decadal Variability to strong tropical volcanic eruptions. Clim. Dyn. 39 (12), 2917–2936.
Xiang, B., Wang, B., Li, T., 2013. A new paradigm for the predominance of standing Central Pacific Warming after the late 1990s. Clim. Dyn. 41, 327–340.
Zanchettin, D., Timmreck, C., Graf, H.-F., Rubino, A., Lorenz, S., Lohmann, K., Krüger, K., Jungclaus, J., 2012. Bi-decadal variability excited in the coupled ocean–atmosphere system by strong tropical volcanic eruptions. Clim. Dyn. 39 (1–2), 419–444.
Zhang, Y., Wallace, J.M., Battisti, D.S., 1997. ENSO-like interdecadal variability: 1900–93. J. Clim. 10 (5), 1004–1020.
Zorita, E., González-Rouco, J., von Storch, H., Montávez, J., Valero, F., 2005. Natural and anthropogenic modes of surface temperature variations in the last thousand years. Geophys. Res. Lett. 32, 8707.